Noninverted images in inferior mirages

Siebren Y. van der Werf

Kernfysisch Versneller Instituut, University of Groningen, Zernikelaan 25, NL-9747 AA Groningen, The Netherlands (vdwerf@kvi.nl)

Received 10 May 2011; accepted 12 June 2011;
posted 29 June 2011 (Doc. ID 147358); published 16 August 2011

Inferior mirages over sun-exposed roads often appear in isolated strips at their near sides and the reflected scenery exhibits multiple images. This effect is explained as due to slight undulations of the road's surface. At the same time, some of these images, although they are reflections, are not inverted. Photographic material illustrates this phenomenon and a ray tracing study is presented that confirms these conclusions. © 2011 Optical Society of America

OCIS codes: 010.1290, 010.4030.

1. Introduction

The most widely known mirage is probably the desert mirage, in the asphalted part of the world now known as the road mirage. On a sunny day, the road's surface and the air immediately above it may easily be hotter by some 20 °C or more than it is only half a meter higher up. This temperature jump produces a density inversion, which causes near-grazing light rays to be bent upward from a negative into a positive slope. In the distance, the road looks as if it were covered with water and the distance of this reflective zone away from the observer is easily found by the following simple argument: the refractivity, $n-1$, of air is proportional to its density, and, by the ideal gas law, the index of refraction for air n may be written as [1]

$$n = 1 + AP/T, \tag{1}$$

where T is the absolute temperature and P is the atmospheric pressure. A is the reduced refractivity, and, for visible light, its numerical value is $7.872 \times 10^{-5}\,\mathrm{K/hPa}$.

An observer at height h above the road will see the near edge of the mirage at a small negative angle $-\beta$ and judge its distance to be $L = h/\tan(\beta) \approx h/\beta$.

By Snell's law,

$$n(h)\cos(\beta) = n(0). \tag{2}$$

Ignoring the height dependence of pressure and assuming the road to be perfectly flat, Eqs. (1) and (2) combine in paraxial approximation to

$$L = h\sqrt{\frac{T(0)T(h)}{2AP[T(0)-T(h)]}}. \tag{3}$$

For $h = 1\,\mathrm{m}$, $P = 1013.25\,\mathrm{hPa}$, $t(h) = 300\,\mathrm{K}$, and $T(0) = 320\,\mathrm{K}$, this distance is estimated at $L \approx 175\,\mathrm{m}$. At distances shorter than this limit, the observer will see the road itself; beyond it, he or she sees reflections of the farther-away scenery.

Figure 1 shows a photograph of a road mirage the author took on April 20, 2011. It was a warm and sunny day with temperatures around 26 °C, and the road itself was about 20° hotter. The near side of the mirage occurs roughly where it would be expected on the basis of the above estimate, but it is fragmented into strips. Closer inspection suggests that these coincide with small depressions of the road's surface, too small to be noticed when driving over it, but visible by the resulting alternation of the slightly convex and concave "mirrors" that they produce. The hollow parts of the road would act as concave mirrors and might produce reflected images, which, at least in part, are upright. Indeed, in Fig. 1, the reflection of the white arrow on the "keep right" sign suggests

0003-6935/11/280F12-04$15.00/0

Fig. 1. (Color online) Road mirage, showing its near side fragmented into strips. Note that the reflection of the white arrow of the "keep right" sign on the traffic island, about 400 m away, seems noninverted. Photograph: Siebren van der Werf, April 20, 2011, Roden, The Netherlands.

that it points downward, as the sign itself does, and is therefore noninverted. However, due to the rapid vibrations in the air just above the road, such images are generally less sharp than the direct image, and capturing a convincing example of a noninverted reflection remains a lucky shot.

In the present work, the author investigates more systematically the hypothesis that the near-side fragmentation of road mirages might be due to undulations of the surface and its possible consequences of finding noninverted images.

2. Results

A. Photographic Material

The collage of pictures in Fig. 2, taken on April 11 and 24, 2011, again in warm weather of about 26 °C, shows the same scenery as Fig. 1. A white pole, 3 m long, has been put up against a street light. It has been set up at an angle so that its reflection will immediately show where the image is upright and where it is inverted. The result is self-evident: the pole's reflection is a zigzag line and where its slope is positive, as that of the pole itself, the image is upright. It is inverted where its slope is negative.

B. Ray Tracing

The effect of undulations in the road's surface may be studied by ray tracing. The surface is given a sinusoidal height profile

$$g(x) = a \sin(2\pi x/D) \tag{4}$$

with amplitude $a = 2$ cm and period $D = 50$ m.

A temperature profile as a function of distance z above the road

$$T(z) = T_0 + \Delta T \exp[-(z-g)/d] \tag{5}$$

is adequate and for this study; ΔT has been chosen 20 °C, with a decay constant $d = 2$ cm. Actual measurements showed that these values are realistic.

Ray tracing was performed along the lines described in earlier publications [2,3]. Figure 3 shows a sample of the rays for an observer at 50 cm above

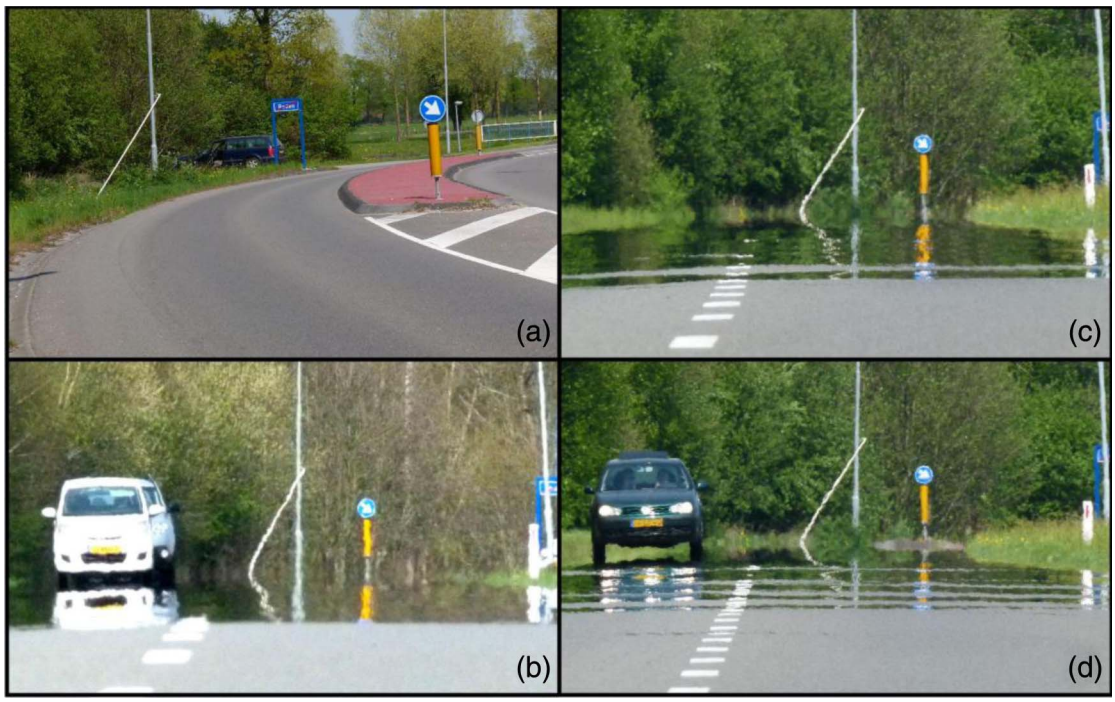

Fig. 2. (Color online) (a) Same road sign as in Fig. 1. Left: a white pole has been put up against a nearby street light. (b) Same scenery from a distance of about 400 m, close to the position from where the picture of Fig. 1 was taken. Camera height: 40 cm. (c) Idem, camera height 50 cm. (d) Idem, camera height 60 cm. Photographs: Siebren van der Werf. (b) April 11, 2011; (a), (c), (d) April 24, 2011.

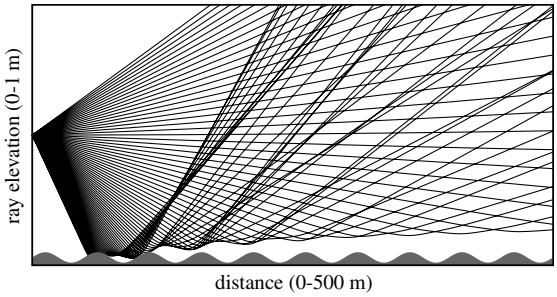

Fig. 3. Ray tracing example over a road surface, which has a sinusoidal undulation with amplitude 2 cm and a period of 50 m. The observer is at 50 cm above the road. The temperature jump is 20 °C, decaying exponentially with a decay constant $d = 2$ cm.

the road. Close to the observer, the rays "see" the undulations and within the concave parts of the road, their upward sweep first diminishes and then increases. The fragmentation of the reflection comes out naturally: via the steepest rays, the observer sees the asphalt. Then follows a reflecting zone in a hollow part of the road, but, near its end, the rays hit the ground again. Farther out, the rays sample less and less the individual undulations but rather sense their integrated profile. This is even better seen in Fig. 4, which shows the height at which the ray crosses a plane 400 m away from the observer, plotted versus the observation angle. This figure also illustrates that the distance of the reflection zone's nearest edge differs from that for a perfectly flat road. Depending on the phase of the sinusoidal undulation, it may either be farther away or closer to the observer, as it is in the parameterization used here. For an undulating road, a part of the curve where backward traced rays hit the road, is missing. Farther away, the transformation curve oscillates and its wiggles show both negative slopes, which correspond to an inverted image, and positive ones, where the images are upright.

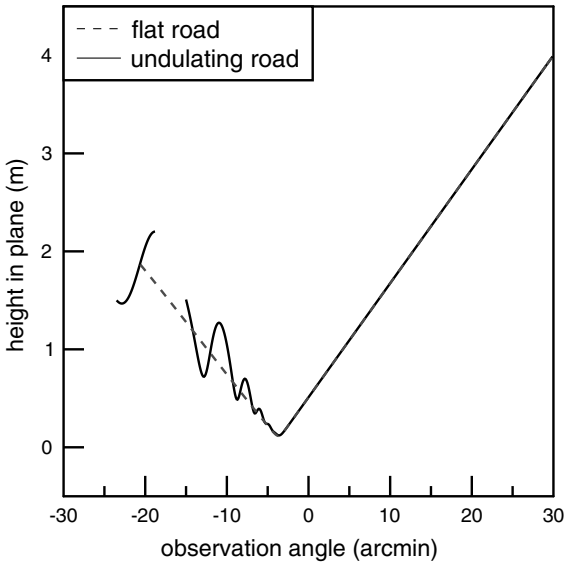

Fig. 4. Height of the ray at a distance of 400 m away from the observer as a function of observation angle.

Based on this transformation curve, Fig. 5 shows by simulation how a 2.5 m long pole would look from 400 m distance when mounted at 45°. Without the undulations (hence, for a perfectly flat road), its reflection would indeed be the perfect inverse of the direct image. However, over an undulating road, a zigzag curved reflection arises, in complete consistency with the photographs in Fig. 2.

C. Schematic Conditions for Producing a Noninverted Image

Consider a horizontal element of the road and let $g(x)$ be its height profile. Then $1/R \equiv d^2g/dx^2$ will be the local curvature. Let an observer at height h and at distance L see a reflection in this road element, as is illustrated in Fig. 6. It is elementary to prove that, in paraxial approximation, a focus exists at a distance L' away from the road element:

$$L' = (hR/2L)\frac{1-(2L/h)dg/dx}{1-(hR/2L^2)}. \tag{6}$$

In the ray tracing example of Fig. 3, this focusing effect is well illustrated by rays that are reflected from the nearest reflecting hollow of the road.

For $L^2 > (hR/2)$ and $dg/dx = 0$, this focus is on the opposite side from the observer and one has a kind of lens formula:

$$\frac{1}{L}+\frac{1}{L'}=\frac{2L}{hR}. \tag{7}$$

At first sight, it would seem that the right-hand side of Eq. (7), and thus the focal length, depends on L. Considering, however, that the reflection is caused by a warm air layer immediately above the ground, and that somewhere just above this road element the ray must be locally horizontal, one has by Eq. (3):

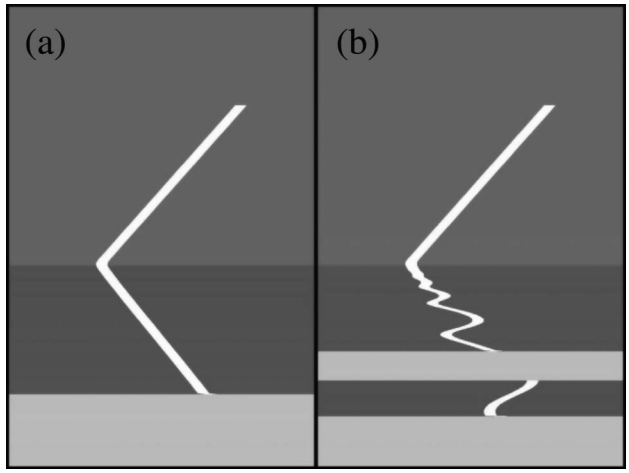

Fig. 5. Simulation of the direct image and the reflection of a 2.5 m long skewed pole over a (a) perfectly flat road and an (b) undulating road as in the present analysis. Note that the nearest reflection zone is at closer distance in the presence of undulations.

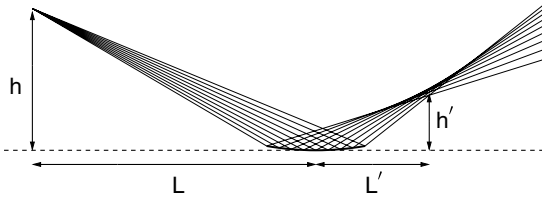

Fig. 6. Illustrating the lens formula for paraxial reflection off a concave road element. Objects beyond a distance $L + L'$ away from the observer are seen upright.

$$\frac{1}{L} + \frac{1}{L'} \approx \frac{2}{R} \sqrt{\frac{T^2}{2AP\Delta T}}, \tag{8}$$

showing that the focal length is independent of L and L'. By Eq. (6), the distance L' is reduced when $dg/dx > 0$, i.e., when the road element has a slight upward slope.

Any scenery farther away from the observer than $(L + L')$ will produce a noninverted image. In particular, an object at distance D behind the reflecting road element, such that

$$\frac{1}{D} = \frac{1}{2}\left[\frac{1}{L'} - \frac{1}{L}\right] \tag{9}$$

is seen at vertical magnification $= 1$: the reflected image has the same vertical extension as in the direct view. This situation is closely met by Fig. 1, where the image of the "keep right" sign is seen upright and at about the same size as the sign itself. The reflection is about 160 m away from the observer and the traffic sign is at 400 m. It is at 1.5 m above the road and the camera was held at about a height of 1 m. From the above formulae, it is estimated that the focus was at 68 m beyond the reflection and that the road's local radius of curvature was about 15 km, meaning a local depression of the road surface of 1.3 cm over 20 m in length. By Eq. (8), the temperature jump above the road is estimated to have been 22 °C.

These schematic estimates corroborate the conclusions based on the photographs and the ray tracing simulations, where the noninverted parts of the reflected image arise mostly from those regions where the road is hollow and upward sloping.

3. Summary and Discussion

It has been shown that a departure from perfect flatness affects the appearance of an inferior mirage over a hot road and that undulations of its surface make the near edge of the mirage appear as a fragmented strip pattern. Consistency is found between photographed mirages and a ray tracing simulation. Perhaps a surprising conclusion is that such undulations make the image appear globally inverted, yet in finer detail consisting of alternating inverted and upright images.

Similar phenomena may occur on a much larger scale. Tränkle [4] has described and analyzed inferior mirages over the Halligen Sea. This region is part of a landscape, named "Watt" in German and "Wad" in Dutch, that stretches all the way along the German Bight, from the north of Holland to above the Danish–German border, bordered to the sea side by a row of islands. At low tide, it falls dry and mirages are frequently seen over the dried-up mud flats and sand plates, which are then intersected by tidal streams. Tränkle reports observations of inferior mirages that show multiple reflections and whose images are, in part, upright. He explains the effect as the result of a warm air layer with two regions of strong negative temperature gradient: one directly above the ground and another higher up, around 1.5 m. Tränkle also shows mirages with horizontal stripes across them, and he interprets these as due to light rays through which the observer sees the ground. He simulates this effect by adding to the temperature profile a term that makes the air cooler where the line of sight crosses a water stream, thus making the isotherms follow the ground profile. This is essentially the same procedure as I have adopted in the present study: the width of the water stream in Tränkle's analysis corresponds roughly to half a period of the sinusoidal road undulation in mine.

The analogy goes further: the present analysis of a road mirage may be scaled up by making the undulations 20 times longer and by increasing their amplitude from 2 to 40 cm. This is quite realistic for dried-up sand plates. The temperature jump above the ground may be lowered as to make the curvature of the light rays 20 times smaller. In this scaled-up version, a double and partly upright mirage emerges naturally and the complication of invoking a two-component warm air layer is avoided. In addition, just as for the road mirage, there is a horizontal strip where the rays hit the ground.

Undulations and curvedness of the road can displace the front edge of the mirage from where the observer would see it over a flat road, and this effect can be drastic. Failure to recognize this phenomenon has led some researchers [5,6] to conclude that it would not be the warm air layer above the road, but rather the asphalt itself that produces the reflections. Reflectivity of rough or roughened surfaces is a relatively new and promising field. Yet, there is no denying the reflective properties of warm air layers and the present study may assist in how to distinguish reflections directly off the road surface from an inferior mirage.

References

1. For parameterizations as a function of wavelength, see, e.g., D. R. Lide, *Handbook of Chemistry and Physics*, 81st ed. (CRC Press, 2000).
2. S. Y. van der Werf, "Ray tracing and refraction in the modified US1976 atmosphere," Appl. Opt. **42**, 354–366 (2003).
3. S. Y. van der Werf, "Comment on 'Improved ray tracing air mass numbers model'," Appl. Opt. **47**, 153–156 (2008).
4. E. Tränkle, "Simulation of inferior mirages observed at the Halligen Sea," Appl. Opt. **37**, 1495–1505 (1998).
5. H. Fakhruddin, "Specular reflection from a rough surface," Phys. Teach. **41**, 206–207 (2003).
6. M. T. Tavassoly, A. Nahal, and Z. Ebadi, "Image formation in rough surfaces," Opt. Commun. **238**, 252–260 (2004).